ELSEVIER

Chemistry and Physics of Lipids
106 (2000) 157–179

CPL
CHEMISTRY AND PHYSICS OF LIPIDS

www.elsevier.com/locate/chemphyslip

Thermotropic and lyotropic properties of long chain alkyl glycopyranosides. Part II. Disaccharide headgroups

H.M. von Minden [a], K. Brandenburg [b], U. Seydel [b], M.H.J. Koch [c], V. Garamus [d], R. Willumeit [d], V. Vill [a,*]

[a] *Institut für Organische Chemie, Universität Hamburg, Martin-Luther-King-Platz 6, 20146 Hamburg, Germany*
[b] *Research Center Borstel, Division of Biophysics, Parkallee 10, D-23845 Borstel, Germany*
[c] *European Molecular Biology Laboratory c/o DESY, Notkestr. 85, D-22603 Hamburg, Germany*
[d] *GKSS Research Centre, Max Planck Straße, D-21502 Geesthacht, Germany*

Received 13 January 2000; received in revised form 4 April 2000; accepted 6 April 2000

Abstract

We have investigated the thermotropic and lyotropic properties of some long chain alkyl glycosides with disaccharide headgroups. The thermotropism was measured with polarising microscopy and additionally the lyotropism with the contact preparation method, Fourier-transform Infrared (FTIR) spectroscopy, X-ray diffraction and small angle neutron scattering. A broad thermotropic as well as lyotropic polymorphism was found. The compounds displayed thermotropic S_A (lamellar) and cubic phases, and the investigation of the lyotropic phase behaviour led to the observation of inverted bicontinuous cubic V_{II} phases, lamellar L_α phases, normal bicontinuous cubic V_I phases, normal columnar H_I phases, normal discontinuous cubic I_I phases and lyotropic cholesteric phases. The phases are discussed with respect to the chemical structures that have been varied systematically to derive structure–property relationships.

Keywords: Alkyl glycopyranosides; Thermotropic liquid crystals; Lyotropic liquid crystals; Cholesteric phases; Cubic phases; Glycolipids

1. Introduction

The observation of a double melting of certain long chain alkyl glucopyranosides, e.g. hexadecyl-β-D-glucopyranosoide (Fig. 1) by Fischer and Helferich (1911) was the first indication of thermotropic liquid crystalline properties in amphiphilic carbohydrates.

These amphotropic molecules form both thermotropic liquid crystalline phases in their pure state upon heating and lyotropic liquid crystalline phases upon addition of a solvent. The first observation of lyotropic behaviour is also related to studies on alkylated carbohydrates while analysing the extracts from tuberculosis bacteria.

* Corresponding author. Tel.: +49-40-428384269; fax: +49-40-428384325.
E-mail address: vill@liqcryst.chemie.uni-hamburg.de (V. Vill).

0009-3084/00/$ - see front matter
PII: S0009-3084(00)00151-1

Koch (1884) observed unusual optical textures of their aqueous dispersions.

The driving force for the mesophase formation in the case of amphiphilic molecules is a micro phase separation leading to an aggregate structure with separated regions for the lipophilic and hydrophilic molecular moieties. This structure enables the maintenance of the van der Waals interaction in the hydrophobic region and of the hydrogen bonding in the hydrophilic region, each stabilising the formed mesophase.

The principal phase behaviour of these compounds is shown in Fig. 2 (Prade et al., 1995; Blunk et al., 1998). A typical amphiphile is represented by a vertical line and usually exhibits only one mesophase, but in the case of an unusual geometry of the hydrophilic headgroup polymorphism can occur. In this case, cubic phases may also be observed (Fischer et al., 1994), while simple amphiphiles such as the one shown in Fig. 1 normally exhibit thermotropically only an S_A phase (Jeffrey and Wingert, 1992).

Deviation from the vertical line mentioned above may also be seen upon the addition of solvents, the most common of which is water, because of its biological relevance. Whereas small amounts of water will not change the phase type and transition temperatures, larger amounts will introduce new phases such as cubic phases and columnar phases ($H_{I/II}$). The discontinuous cubic phases are based upon various packings of spherical or slightly anisotropic micelles, whereas the bicontinuous cubic phases with interwoven fluid porous structures are based upon underlying infinite periodic minimal surfaces (Fairhurst et al., 1998).

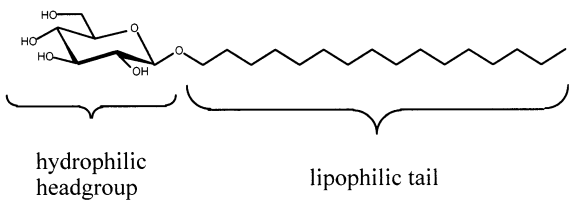

Fig. 1. Hexadecyl-β-D-glucopyranoside.

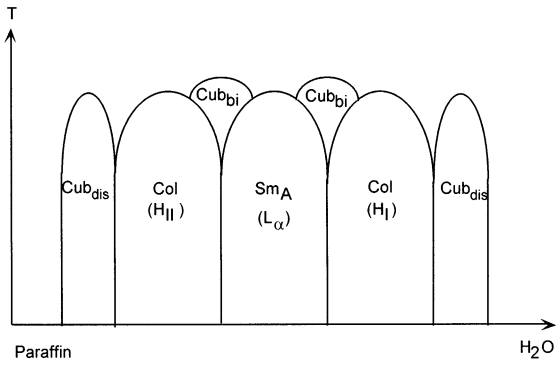

Fig. 2. Principal phase behaviour of amphiphilic compounds.

This phase in particular is of great biological interest (Siegel, 1986a,b,c; Siegel et al., 1989; Ellens et al., 1989; Lindblom and Rilfors, 1989). The lamellar phase with its multibilayer structure has long been well known to the biologists, but there is much evidence today that the bicontinuous cubic phase may play an important role in processes such as membrane fusion.

Whereas the first observation of liquid crystalline properties of alkylglycosides was related to long chain compounds, subsequent interest focused only on their shorter chain counterparts (Jeffrey, 1984; Jeffrey and Wingert, 1992; Prade et al., 1995) because of their interesting properties as surfactants (Böcker and Thiem, 1989; Vill et al., 1989; Boullanger, 1998). These compounds dissolve in water, whereas the long chain glycosides do only swell.

We synthesised long-chain alkyl glycopyranosides (in particular stearyl glycosides) which can be incorporated in biomembranes, and change the sugar headgroup systematically to elucidate the structure–property relationships governing the occurrence of the polymorphism mentioned above. In the case of a disaccharide headgroup, we observed a broad range of phases.

2. Materials and methods

2.1. Materials

General reaction conditions were as follows. The alkyl glycosides had been synthesised as shown in Fig. 3 for the cellobiosides using the method described by Vill et al. (1989), however

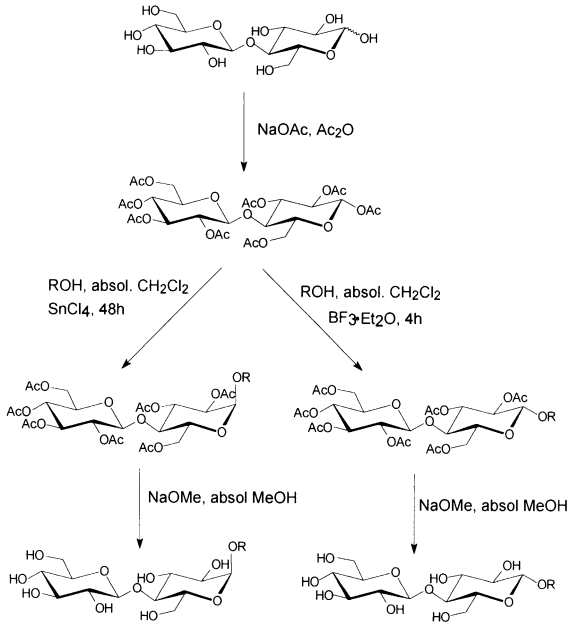

Fig. 3. Synthesis of alkyl glycopyranosides.

boron trifluoride diethyl etherate was used instead of tin tetrachloride as Lewis acid for the synthesis of the β-anomers. Furthermore, no ion exchange chromatography was necessary in our case to separate the anomers, since a silica gel chromatography [light petroleum (b.p. 60–70°C)–ethyl acetate 4:1] was already successful, while in the case of the homologous dodecyl glycosides prepurification by silica gel chromatography and a subsequent ion exchange chromatography after deprotection on Dowex 1 × 2 has been used (Rosevar et al., 1980; Böcker and Thiem, 1989). For further information concerning the synthesis and characterisation, please contact the author of correspondence.

2.2. Methods

An Olympus BH optical polarising microscope equipped with a Mettler FP 82 hot stage and a Mettler FP 80 central processor was used to identify thermal transitions and characterise anisotropic textures.

2.2.1. Sample preparation for lyotropic phase behaviour

The glycolipid samples were prepared as aqueous dispersions at 90% buffer content using 20 mM Hepes, in some cases at lower water content (50%) also. For this, the lipids were directly suspended in the buffer, and the suspensions were temperature-cycled several times between 5 and 70°C and then stored for at least 12 h at 4°C before measurement.

2.2.2. FTIR spectroscopy

Infrared spectroscopic measurements were performed on FTIR spectrometers '5-DX' (Nicolet Instruments, Madison, WI) and IFS-55 (Bruker, Karlsruhe, Germany). The lipid samples were placed in a CaF_2 cuvette separated by a 12.5-μm thick teflon spacer. Temperature scans were performed automatically between 10 and 70°C with a heating rate of 3°C per 5 min. Every 3°C, 50 interferograms were accumulated, apodised, Fourier-transformed, and converted to absorbance spectra. The gel to liquid crystalline phase transition $L_\beta \leftrightarrow L_\alpha$ (S_B to S_A in lamellar phases) was determined by evaluating the symmetric stretching vibration of the methylene groups $\nu_s(CH_2)$ with standard procedures. The location of $\nu_s(CH_2)$-around 2850 cm^{-1} in the gel phase and 2853 cm^{-1} in the fluid phase — is a sensitive indicator of acyl chain order (Casal and Mantsch, 1984).

2.2.3. X-ray diffraction

X-ray diffraction measurements were performed at the European Molecular Biology Laboratory (EMBL) outstation at the Hamburg Synchrotron Radiation Facility HASYLAB using the double-focusing monochromator-mirror camera X33. Diffraction patterns in the range of the scattering vector $0.07 < s < 1$ nm^{-1} ($s = 2 \sin \theta/\lambda$, 2θ the scattering angle, and λ the wavelength = 0.15 nm) were recorded at 40°C with exposure times of 2 or 3 min using a linear detector with delay line readout (Gabriel and Dauvergne, 1982). The s-axis calibration was done using tripalmitin as standard (periodicity 4.06 nm at 25°C). Further details of the data acquisition and evaluation system can be found

elsewhere (Boulin et al., 1986). In the diffraction patterns presented here, the logarithm of the diffraction intensities $\log I(s)$ is plotted against the scattering vectors. The evaluation of the X-ray spectra was made according to procedures described by Luzzati et al. (1986) and in previous papers (see Brandenburg et al., 1990, 1998) which allow the assignment of the spacing ratios of the main scattering maxima to defined three-dimensional structures. Here lamellar and cubic structures are of particular relevance, which can be characterised by the following features.

1. Lamellar (smectic phases)
   The reflections are grouped in equidistant ratios, i.e., at 1, 1/2, 1/3, 1/4 etc. of the lamellar repeat distance d_l.
2. Cubic
   These are non-lamellar three-dimensional structures. Their various space groups differ in the ratio of their spacings. The relation between reciprocal spacing $s_{hkl} = 1/d_{hkl}$ and lattice constant a is $s_{hkl} = (h^2 + k^2 + l^2)^{1/2}/a$ (hkl = Miller indices of the respective set of plane).

In addition, X-ray wide-angle diffraction was performed in selected cases, in which the determination of the short-range order is possible. In the case of a hexagonal array of the lipid chains such as found for many phospholipids, the distance between neighbouring acyl chains, the lattice constant a, can be calculated from the main wide-angle reflection at a spacing ratio d by $a = 2/\sqrt{3}d$.

2.2.4. Small angle neutron scattering

A set of small-angle neutron scattering experiments was performed on the SANS1 instrument at the FRG1 research reactor of GKSS, Geesthacht, Germany (Stuhrmann et al., 1995). The range of scattering vectors q from 0.0008 to 0.025 nm^{-1} was covered by three combinations of neutron wavelength (0.85 nm) and sample-to-detector distances (from 0.7 to 7 m). The wavelength resolution was 10% (full-width-at-half-maximum value).

The samples were kept in quartz cells with a path length of 1.5 mm at 23°C. The raw spectra were corrected for backgrounds from the solvent, sample cell, and other sources by conventional procedures (Stuhrmann, 1989). The two-dimensional isotropic scattering spectra were azimuthally averaged, converted to an absolute scale, and corrected for detector efficiency by dividing by the incoherent scattering spectra of pure water (Wignall and Bates, 1986) which was measured with a 1-mm-path-length quartz cell.

2.2.5. SANS analysis

2.2.5.1. Model-independent approach. The pair distribution function, $p(r)$, of scattering length density of studied micelles is in principle obtained by Fourier transformation of the measured difference cross-section of neutron scattering. The overall shape and dimensions of the micelles can in many cases be estimated from the pair distribution function (Glatter and Kratky, 1982.). As the scattering is only measured in a finite q range, a traditional Fourier transformation cannot be performed. Instead, the method of indirect Fourier transformation is used (Glatter, 1977; Pedersen, 1997).

Having determined $p(r)$ we are able to calculate integral parameters of the micelle (Glatter, 1992) such as the radius of gyration R_g.

2.2.5.2. Modelling. The difference cross section of neutron scattering of the population of non-interactive particles (Glatter and Kratky, 1982) can be written as

$$\frac{d\Sigma(q)}{d\Omega} = \frac{d\Sigma(0)}{d\Omega F^2(q) + B_{inc}},$$

where $d\Sigma(0)/d\Omega$ is the scattering at 'zero' angle and is related to concentration of particles, volume and difference of scattering length densities between particle and solvent, B_{inc} is the residual incoherent background. The form factor $F(q)$ expresses the scattering cross section of particle. In the case of particle of ellipsoidal or cylindrical shape (Pedersen, 1997), it is written as

$$F^2(q) = \int_0^{\pi/2} [f(q,\beta)]^2 \sin\beta d\beta$$

In the case of a homogeneous cylinder $f(q, \beta)$ is written as

14	Cr	151.7				S_A	283.5	I, b
16	Cr	181.4	(cub	178.0)		S_A	260.2	I
18	Cr	183.0	(cub	181.5)		S_A	284.0	I
20	Cr	129.8				S_A	252.0	I
22	Cr	152.0				S_A	262.0	I
24	Cr	169.2	(cub	163.0)		S_A	268.0	I
26	Cr	90.5	cub	151.0		S_A	160.5	I
28	Cr	155.0	(cub	137.0)		S_A	171.0	I
30	Cr	152.0	cub	157.0		S_A	168.0	I
32	Cr	?	non mesogenic					
34	Cr	120.0	X	96.0	cub	138.0	S_A	154.0 I, c

Fig. 4. (*Continued*)

$$f(q,\beta) = \frac{\sin(qL/2\cos\beta)2J_1(qR\sin\beta)}{(qL/2\cos\beta)(qR\sin\beta)},$$

where L is the length of the cylinder, R is the radius of the cylinder, J_1 is the first-order Bessel function, and β is the angle between the **q** vector and the axis of the cylinder.

In the case of an ellipsoid of rotation with semi axis R, R, εR $f(q, \beta)$ is written as

$$f(q,\beta) = \frac{3[\sin(x) - x\cos(x)]}{(x)^3}$$

where $x = qR[\sin^2\beta + \varepsilon^2\cos^2\beta]^{1/2}$.

The models mentioned above were applied to fit experimental data.

3. Results and discussion

3.1. Thermotropic phase behaviour

Fig. 4 depicts a systematic structure variation of octadecyl-β-D-glucopyranoside **2**. While the first part of this paper (Vill et al., 1999) focussed on long chain alkyl glycopyranosides with monosaccharide headgroups, we present here re-

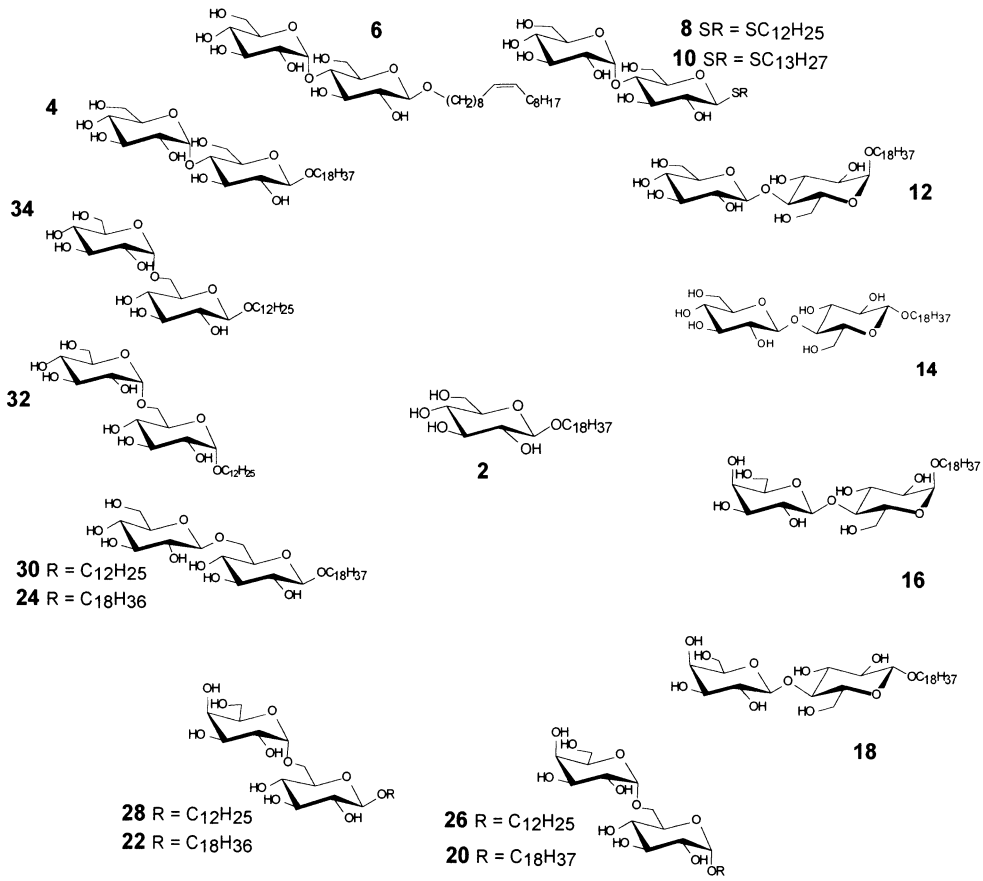

2	Cr_2	87.0	Cr_1	93.3		S_A	146.8 I
4			Cr	106.0		S_A	274.0 I,
6			g	?		S_A	267.0 I, a
8			Cr	135.7		S_A	246.2 I
10			Cr	139.0		S_A	260.0 I
12			Cr	130.0	(cub 127.4)	S_A	263.0 I

Fig. 4. Thermotropic behaviour of the synthesised amphiphilic liquid crystals; (a) the compound formed a glass and, thus, no melting point could be determined; (b) the synthesis of this compound and the rough transition temperatures without a characterisation of the phase type were reported first bei Hori (1958); (c) an additional (probably columnar) metastable mesophase was formed on cooling.

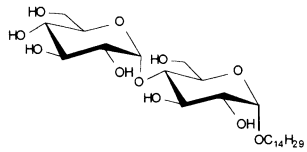

41	Cr	?[a]	S_A	231.0	I

Fig. 5. (*Continued*)

sults obtained by replacing the monosaccharide moiety of compound **2** by disaccharides.

If the glucose headgroup of compound **2** is replaced by the α 1→4-linked disaccharide unit of maltobiose (compound **4**), the clearing temperature increases dramatically by 127 K due to increased hydrogen bonding in the headgroup region attributable to the increased number of hydroxyl groups. Furthermore, a better ratio between the polar and unpolar moieties is obtained by exchanging the glucose headgroup of **2** for a disaccharide unit. The optimal hydrophilic/hydrophobic balance and, therefore, the highest clearing temperature is reached in the case of monosaccharide headgroups with a chain of 12–14 carbon atoms (Prade et al., 1995). However, the optimal balance between the hydrophilic and hydrophobic moieties is reached in case of disaccharide headgroups at longer chain length.

The introduction of a unsaturation in compound **6** again lowered the clearing temperature, but with only 7 K less than in the case of the monosaccharide derivatives described in part I of this paper. The reason for the lower clearing temperatures of the unsaturated derivatives in general can be seen in the disturbance introduced into the alkyl chain region by the double bond, circumventing a close packing of the alkyl chains and, therefore, lowering the van der Waals interactions. The stronger effect of the unsaturation on the monosaccharide derivatives with an already imbalanced ratio between the polar and unpolar molecular moieties might be explained by the broadening of the alkyl chains introduced through the unsaturation, increasing the hydrophobic volume and hence the imbalance even further. However, there is still a more general explanation: it seems that the effect of structural changes in the aliphatic chain on the clearing temperature are stronger in the case of monosaccharide headgroups than in the case of disaccharide headgroups. An interesting observation, which further supports this hypothesis, is that of the effect on the clearing temperature, if the oxygen is replaced by sulphur as linking atom between the hydrophilic and hydrophobic moieties of a maltobioside. In the case of α-D-thioglucosides (Van Doren et al., 1989) [unfortunately insufficient data are available about the β-D-thioglucosides] and also in the case of many other thio compounds with a monosaccharide headgroup-e.g. the 1-thioglycerides (Van Doren et al., 1990), 1-alkylthio-1-deoxy-D-glucitols (Dahlhoff, 1990), thioesters of galacturonic acid (Vogel et al., 1992) and dialkyl thioacetals of D-glucose (Dahlhoff, 1987; Eckert et al., 1987; Van Doren et al., 1988; Tietze et al., 1994), the thio derivatives always exhibit distinctly higher clearing temperatures than the oxygen-linked derivatives. Nevertheless, the dodecyl thio maltobioside **8** exhibits nearly the same clearing temperature as the oxygen-linked maltobioside (compound **35**, Fig. 5) and proves, therefore, our hypothesis. For other reasons, we also synthesised the tridecyl thio maltobioside **10** with a clearing temperature of 260.0°C. Unfortunately, no literature data are available on the clearing temperature of the analogous oxygen-linked compound, but we calculated a value of 254.5°C using LiqCryst data base (Vill, 1999). This value seems reasonable, since the maltobiosides do not show an odd–even effect, and the calculated temperature should, thus, lie in the middle of the clearing temperatures of the dodecyl and tetradecyl maltobioside (Fig. 5, compounds **35** and **36**). This tem-

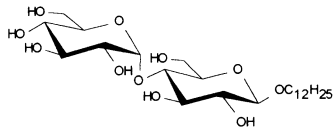

35 Cr 102.0 S_A 245.0 I

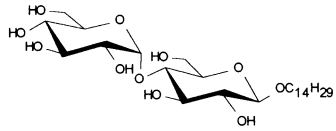

36 Cr 107.0 S_A 264.0 I

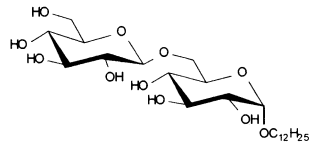

37 Cr ?[a] cub 158.0 I

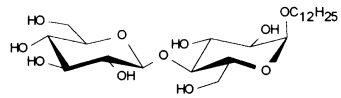

38 Cr ?[a] S_A 224.0 I

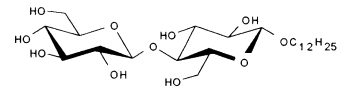

39 Cr ?[a] S_A 259.4 I

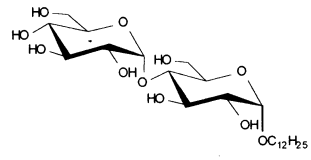

40 Cr ?[a] S_A 205.0 I

Fig. 5. Literature data for the transition temperatures of some amphiphilic liquid crystals for comparison; (a) in the literature no exact melting point was given, since the compounds formed non-crystalline solids after lyophilisation.

perature is again only slightly lower than the clearing temperature of the thio derivative **12**.

In the next step, we changed the type of the interglycosidic linkage (α vs. β), the position of linkage (1→4 vs. 1→6), and the configuration of the second sugar residue (glucopyranosyl vs. galactopyranosyl) systematically. The clearing temperatures of these compounds varied over a range of 33 K owing to the various kinds of configurations, and in several cases cubic phases were found.

3.1.1. Influence of the type of linkage (α vs. β) of the aliphatic chain to the disaccharide headgroup

In all these cases, the compounds with the aliphatic chain linked by a β glycosidic bond (compounds **14**, **18**, **22**, **28**, **30** and **34**) to the disaccharide moiety displayed a higher clearing temperature (and also the higher m.p.) and, hence, the more stable smectic A phase than the corresponding α anomer (**12**, **16**, **20**, **26**, **37** and **32**). This difference in stability was in the case of compounds with disaccharide headgroups with a interglycosidic 1→6 linkage with about 10 K (compounds **22**, **28**, **30** and **34** vs. **20**, **26**, **37** and **32**) smaller than in the case of the compounds with the two glycosyl units of the disaccharide headgroup being linked by a 1→4-linkage (about 20 K, compounds **14** and **18** vs. **12** and **16**). The reason for the greater stability of the compounds with a β-anomerically-linked aliphatic chain might be seen in their somewhat more rod-like shape. This effect is not so strong in the case of compounds with a 1→6-linked disaccharide unit, since the sugar moiety is angular and causes the molecule already to be banana-shaped. This deviation from a rod-like structure is much stronger than the one introduced by an α linkage of the aliphatic chain to the sugar moiety, and a further deviation from a rod like structure due to the latter, therefore, decreases the stability of the S_A phase only slightly.

While this difference in stability between the two anomers is more or less chain-length independent in case of a 1→6-linked headgroup (melibiosides, **22** and **28** vs. **20** and **26**), it is strongly dependent on the chain length in case of compounds with a 1→4-linked disaccharide headgroup. The difference in stability between the two anomers is in case of the cellobiosides, e.g.

cel-β-OC18 (**14**)	vs. cel-α-OC18 (**12**)	20.5 K
cel-β-OC12 (**39**)	vs. cel-α-OC12 (**38**)	35.4 K

and similar results are found for the maltobiosides,

mal-β-OC14 (**36**)	vs. mal-α-OC14 (**41**)	33 K
mal-β-OC12 (**35**)	vs. mal-α-OC12 (**40**)	40 K.

3.1.2. Influence of the type of linkage between the two sugar residues (α vs. β)

If the α 1→4-linked second glucopyranosyl residue of the maltoside **4** is replaced by a β 1→4-linked glucopyranosyl residue (cellobiosides **14**), the clearing temperature increases by 9.5 K due to the stiffer and more rod-like structure of the cellobioside headgroup. This difference in stability also increases again with decreasing chain length as can be seen easily from the data in Fig. 5.

Whereas the maltobiosides displayed only smectic phases, the α cellobioside **12** displays a monotropic cubic phase (see also Table 1), which could not be found in the case of the β cellobioside **14**, since on cooling of the S_A phase crystallisation occurred already some degrees below the melting point. These results will be discussed together with the lactosides in the following section.

3.1.3. Influence of the configuration of the second sugar residue (glucopyranosyl vs. galactopyranosyl)

If the second, β 1→4-linked glucopyranosyl residue of the cellobiosides **12** and **14** is replaced by a β 1→4-linked galactopyranosyl residue, the stability of the S_A is more or less not effected; the clearing temperature of the α lactoside **16** is 2.8 K lower than the clearing temperature of the corresponding α cellobioside while the clearing temperature of the β lactoside **18** is 0.5 K higher than in the case of the β cellobioside. The configuration at C-4 of the second sugar moiety seems to have, therefore, more or less no influence on the stability of the S_A phase in the case of 1→4-linked

disaccharide headgroups, but this is not true in the case of 1→6-linked disaccharide headgroups (see below).

The α lactoside **16** as well as the β lactoside **18** displayed, as did the α cellobioside **12**, a monotropic cubic phase. The introduction of the galactopyranosyl residue improved in case of the β lactoside compared to the β cellobioside the supercoolability and inhibited the crystallisation, which prevented the occurrence of a monotropic cubic phase of the β cellobioside **14**. So far, only a few sugar derivatives are known to show a thermotropic cubic phase (e.g. Praefcke et al., 1990; Fischer et al., 1994; Beginn et al., 1997; Borisch et al., 1997Borisch and Diele, 1997) and one of them is the dodecyl-α-D-gentobioside **37** (Fischer et al., 1994), some homologous compounds of which have been synthesised in this work and will be discussed below. The occurrence of cubic phases might be attributable in these cases to their banana-shaped molecular structures, whereas the occurrence of thermotropic cubic phases in the case of cello- and lactobiosides is rather unexpected and difficult to explain, since compounds of this type are so far only known to form S_A phases according to our knowledge (Jeffrey and Wingert, 1992; Prade et al., 1995). Because of their rod-like molecular shape they are indeed something like the prototype of S_A phase forming-amphiphilic glycosides.

The exact structure of the headgroup seems to have an influence on the occurrence of this monotropic cubic phase (even if it cannot be understood yet), since the α cellobioside **12**, the α and β lactobiosides **16** and **18**, and the β gentobioside **24** exhibited a monotropic cubic phase while it was not found in the case of the β maltobiosides **4** and **6** and the α and β melibiosides **20** and **22**. At present, only two very general structural requirements can be derived,

- a disaccharide headgroup seems to be necessary, since the similar stearyl gluco- and galactopyranosides (see first part of this paper) did not show this unusual mesogenic behaviour
- a chain of sufficient length is also necessary, since e.g. the homologous dodecyl cellobiosides or tetradecyl lactosides (Vill et al., 1989) only displayed a S_A phase.

Rod-like amphiphilic molecules are known to display a S_A phase, the stability of which increases the more balanced the ratio between the polar and apolar moieties becomes, and decreases afterwards again. If this imbalance between the hydrophilic and hydrophobic moieties is increased sufficiently, a cubic phase might be observed instead of the S_A phase usually found. These findings are similar to the results obtained earlier with some glucamine derivatives (sodium salts of *N*-alkyl-*N*-carboxymethyl-D-glucamine, Vill et al., 1992), but it is still impossible to explain the

Table 1
Gel to liquid crystalline phase transition T_c, type of supramolecular aggregate structures (L lamellar, Q cubic, and H hexagonal), and position of wide-angle X-ray diffraction for various 'glu–glu' and 'glu–gal' glycolipids

Glycolipid	T_c (°C)	Aggregate structures	Wide-angle reflection (nm)
Mel-β-OC12 **26**		L	No reflection
Mel-β-OC12 **28**	<0	L	No reflection
Mel-β-OC18 **20**	38	Q(5–40°C) L/unknown (60–80°C)	0.451, unsharp
Mel-β-OC18 **22**	67.5	L	n.m.
Mal-β-SC12 **8**	<0	L (5–4°C) L/L' interdigitated (60–80°C)	No reflection
Mal-β-SC13 **10**	6	L	0.441 and 0.256
Mal-β-OC18 **4**	40	$H_I > L > Q$	0.424 (5°C), 0.420 (20–40°C)
Mal-β-OC18:1 **6**	<0	L	No reflection
Cel-β-OC18 **12**	36 (T_{pre}) 56	Q (5–60°C), L(80°C)	0.466 and 0.390
Cel-β-OC18 **14**	70	L	n.m.
Lac-β-OC18 **16**	53(T_{pre}) 70	L	0.442
Lac-β-OC18 **18**	78	L	0.453, unsharp
Gen-β-OC18 **24**	54	L(5–60°C), H_{II} (80°C)	n.m.

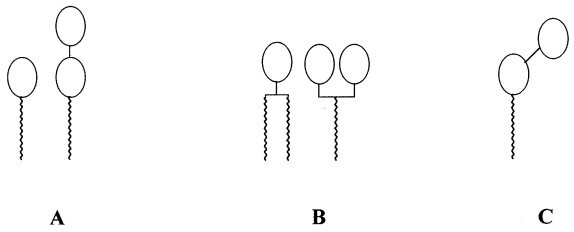

Fig. 6. Types of amphiphiles.

influence mentioned above of the sugar headgroup.

3.1.4. Influence of the position of the linkage between the two sugar moieties in the disaccharide headgroup (1→6 vs. 1→4)

While the 1→4-linked disaccharides are always more or less linear, the 1→6-linked disaccharides are generally angular, yielding a banana-shaped structure of the glycosides made thereof, which influences their mesogenic behaviour strongly. The stability of the S_A phase is reduced due to the deviation from a rod-like shape as can be seen from a comparison with the transition temperatures of the analogous 1→4-linked derivatives. The extent to which the stability of the S_A phase is reduced depends strongly on the length of the alkyl chain e.g.

gen-β-OC18 (**24**) vs. cel-β-OC18 (**14**): 15.5 K

mel-β-OC18 (**22**) vs. mal-β-OC18 (**4**): 12.0 K

(because an exchange of the second glucopyranosyl residue in the cellobioside for a galactopyranosyl residue did not effect the clearing temperatures, it seems possible to compare the melibiosides with the maltobiosides instead of comparing with the proper compounds with a disaccharide headgroup of a galactopyranosyl residue linked by an α 1→4 bond to a glucopyranosyl residue)

gen-β-OC12 (**30**) vs. cel-β-OC12 (**39**): 91.4 K

mel-β-OC12 (**28**) vs. mal-β-OC12 (**35**): 74.0 K

isomal-β-OC12 (**34**) vs. mal-β-OC12 (**35**):

91.0 K

The most obvious difference between the glycosides with a 1→6- and a 1→4-linked disaccharide headgroup is the more or less abundant occurrence of cubic phases in the former case. Except for the dodecyl-α-isomaltoside **32**, all of the dodecyl glycosides (**26**, **28**, **30**, **34** and **37**) with a 1→6--linked disaccharide headgroup exhibit a cubic mesophase. Since the α melibioside **26** showed a cubic mesophase while the α isomaltoside **32** did not, this difference in the mesogenic behaviour must be attributed to the changed configuration at C-4 of the second sugar residue due to the exchange of a galactopyranosyl for a glucopyranosyl residue.

The occurrence of a cubic mesophase might be explained in these cases by the broad structure of the 1→6-linked disaccharide headgroups, giving the molecules a banana-shaped structure (this term has been used before by Takezoe (Niori et al., 1996) to describe the molecular shape of a completely different class of symmetric non-carbohydrate liquid crystals with different properties than the compounds discussed here).

Compounds of the general structure **A** (Fig. 6) have so far only been reported to display smectic phases (Jeffrey and Wingert, 1992; Prade et al., 1995), and compounds of type **B** show columnar phases with the interfacial area being curved around the minor component (Mannock et al., 1987, 1990 Jeffrey and Wingert, 1992; Prade et al., 1995). In the case of compounds of type **C**, the headgroup prefers a columnar structure while the aliphatic tail favours a smectic structure, but each is destabilised by the other moiety. The discussed glycosides with a 1→6-linked disaccharide headgroup belong to this last group, which as a result of frustration forms cubic mesophases as a compromise. The cubic to S_A transition may be attributed to the increasing thermal motion in the alkyl chains, leading to a greater effective volume of the hydrophobic chain. This causes the molecule to become rod-like at elevated temperatures and, hence, a cubic to S_A transition is found.

If the dodecyl chain is extended, as in the case of the stearyl melibiosides (**20**, **22**), only an S_A phase is observed, whereas the stearyl gentiobioside **24** displays a monotropic cubic phase. This difference in behaviour might be explained

by the difference in size of the sugar headgroups. With the melibiose headgroup, the stearyl glycosides apparently have a rod-like shape at all temperatures, whereas in the case of the gentio bioside it becomes rod-like at elevated temperatures only.

These two cubic phases (the one observed with banana-shaped short chain molecules and the one observed with long chain glycosides) probably belong to two different groups as might be concluded from the contact preparations with water (see below), the former to the normal type of bicontinuous cubic phases and the latter to the inverted type. These terms are normally only used to describe the structure of lyotropic cubic mesophases, but it seems likely that they can be extended to describe these structures. X-ray investigations and model simulations performed earlier to investigate the structure of the cubic mesophase of dodecyl-α-D-gentiobioside **37** (Fischer et al., 1994) point towards a cubic phase of the space group No. 230, Ia3d, made up by a network of cylinders like in the lyotropic case.

At the end of this section, it seems useful to summarise the results of the discussion of the thermotropic properties.

- The disaccharide derivatives show generally higher melting and clearing points due to the increased hydrogen bonding in the headgroup region.
- The influence of structural changes to the aglycon is diminished in the case of disaccharide derivatives compared with the monosaccharide compounds.
- The stability of the S_A phase increases, the more rod-like the sugar headgroup becomes, generally favouring the β linkage of the saccharide moiety to the aliphatic chain as well as the β linkage between the two glycosyl residues. For the same reason, the stability of the S_A phase of compounds with a $1\rightarrow6$-linked disaccharide moiety is decreased compared with their counterparts with a $1\rightarrow4$-linked disaccharide headgroup.
- The difference mentioned above in stability between the anomers decreases with increasing length of the aliphatic chain.
- There are two different structural features which support the occurrence of thermotropic cubic mesophases,
  - linear structures with an extremely imbalanced ratio between the hydrophilic and hydrophobic moieties may form monotropic cubic mesophases.
  - extremely bent molecular structures, as they are found in glycosides with a $1\rightarrow6$-linked disaccharide moieties, form cubic mesophases in the case of an appropriate length of the aliphatic chain.

3.2. Lyotropic phase behaviour

3.2.1. Structural lyotropism

Above the critical micellar concentration (CMC), glycolipids form supramolecular aggregates in aqueous media. The type of aggregate structure can be assumed to play a biologically relevant role and is determined by the conformation (shape) of the contributing molecules, which is determined by their primary chemical structure and is influenced by ambient conditions such as pH and concentration of mono- and divalent cations (Israelachvili, 1991). Moreover, the molecular shape of a given glycolipid molecule depends on the state of order of the chains, which can assume two main phase states, the gel (β-phase) and the liquid crystalline (α-phase) states. Between these two-phase states, a reversible transition can take place at a given phase transition temperature T_c. The value of T_c is dependent in the first place on the number, length, and degree of saturation of the acyl chains, the conformation and the charge density and its distribution within the headgroup region, and the nature and size of the saccharide moiety. A closer characterisation of the main types of supramolecular aggregate structures (micellar, lamellar L, cubic Q and inverted hexagonal H_{II}) occuring in glycolipid:water systems is given by (Curatolo, 1987). More general information about structural polymorphism can be found elsewhere (Luzzati et al., 1986; Seddon, 1990; Israelachvili, 1991; Seydel et al., 1993). A comprehensive overview of the phases and phase transitions (including the three-dimensional aggregate structures L, Q, and H_{II}) adopted

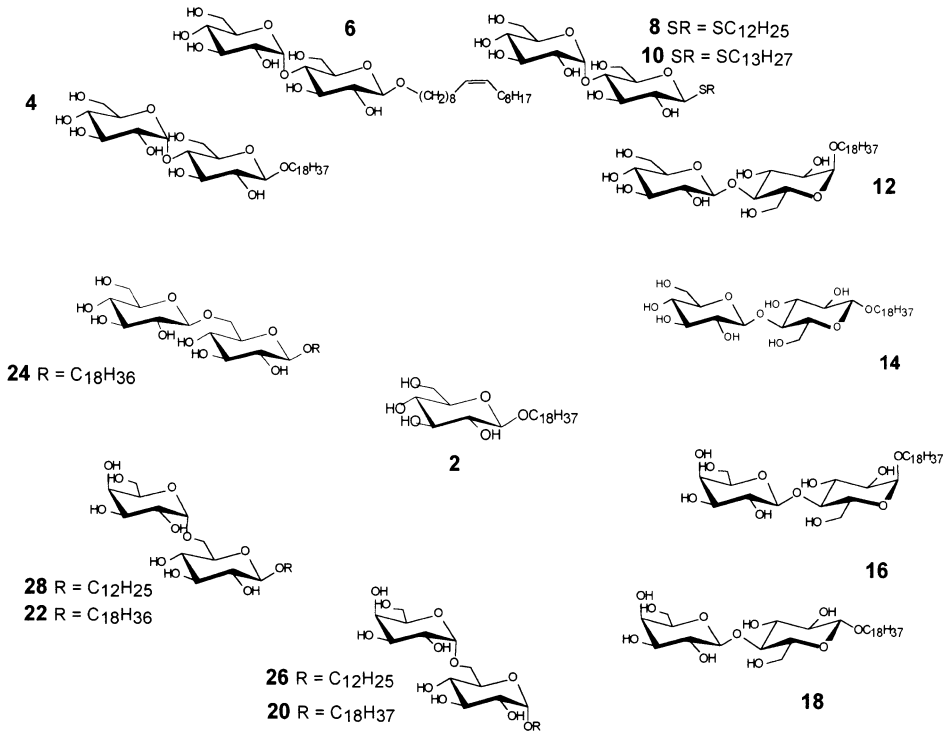

2		Myeline figures			
4		L_α	H_I		ch
6		L_α	V_I	H_I	ch
8		L_α	V_I	H_I	ch
10		L_α	V_I	H_I	ch
12	V_{II}	L_α	V_I	H_I	ch
14		L_α		H_I	ch
16		glass[a]	V_I	H_I	(ch?[b])

Fig. 7. Phase sequences observed in the contact preparation of the synthesised amphiphilic liquid crystals with water; (a) a cubic glass was formed on cooling of the melted sample, which was used for the contact preparation; (b) the boundary of the H_I phase towards the water region was somewhat diffuse, thus, the existence of a lyotropic cholesteric phase could not be proved without doubts.

by glycoglycerolipids is given by Koynova and Caffrey (Koynova and Caffrey, 1994).

The formation of lyotropic phases was investigated by means of X-ray diffraction, small-angle neutron diffraction and the contact preparation technique (Van Doren and Wingert, 1994). If water penetrates the sample, one or more lyotropic phases are formed, which can be identified by polarising microscopy based on their characteristic textures. Because a gradient of water concentration is generated, the whole range of phases starting from the anhydrous bulk in the middle to the completely hydrated sample at the outermost region can be observed. Depending on the position of a particular phase with respect to the other phases, it is even possible to classify it tentatively as belonging to the normal or inverted type in the case of cubic or columnar phases; for the same reason, it is possible to differentiate between a bicontinuous and a discontinuous (micellar) cubic phase. For example, a cubic phase, observed at a higher water concentration than the lamellar phase and followed by a columnar phase should be of the normal bicontinuous type.

The stearyl-β-D-glucopyranoside **2** displayed in a contact preparation with water only myelin figures as did other long chain alkyl glycosides with a monosaccharide headgroup (see first part of this paper; Vill et al., 1999). Myelins are mobile tubular structures, which are considered to consist of cylindrical or helical arrangements of many (300–5000) of the bilayers that constitute the lamellar phase (Jeffrey and Wingert, 1992; Bouligand, 1998).

If the monosaccharide headgroup of **2** is replaced by the disaccharide maltobiose (compound **4**), three phases are formed with increasing water concentration, a lamellar L_α phase; a columnar H_I phase; and a further, only weakly anisotropic phase. Replacing the stearyl chain by an oleyl chain (**6**) leads to the appearance of an additional broad bicontinuous cubic V_I phase, and this phase sequence, i.e. L_α, V_I, H_I, and a weakly anisotropic phase, is also found in the case of the dodecyl- and tridecyl thiomaltosides **8** and **10**. The already mentioned weakly anisotropic phase, which appeared as a more or less thin band at the edge of the H_I phase towards the water region, was also found with all other compounds except for the dodecyl α and β melibiosides **26** and **28** (Fig. 7). Since a micellar cubic I_I phase can be ruled out as explanation because of its isotropic structure, a lyotropic cholesteric phase might be supposed as explanation. This phase is expected to appear at higher water concentration than the columnar H_I phase, and to be anisotropic. Both of these crite-

18		glass[a]	V_I	H_I		(ch?[b]),
20	L_α	Cr	V_I	H_I		ch
22	L_α	Cr		H_I		ch
24		glass[a]	V_I	H_I		ch
26			V_I	H_I	I_I	I_{I^*}
28			V_I	H_I	I_I	

Fig. 7. (*Continued*)

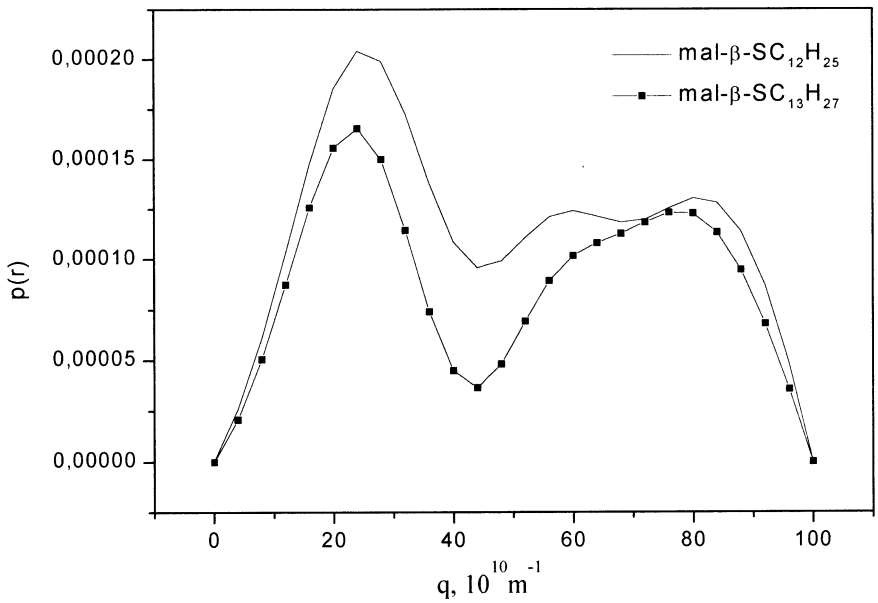

Fig. 8. Distance distribution function $p(r)$ calculated from the experimental SANS data. The experimental solutions were prepared by dissolving the maltobiosides **8** and **10** in heavy water at a concentration of 90 mmol and 100 mmol, respectively.

ria are fulfilled by the phase that has been found. Whereas quite a lot is known about thermotropic cholesteric phases, their lyotropic counterparts are still seldom observed and not well understood. The mesophase of lyotropic cholesteric phases is built up by anisotropic micelles.

The size and shape of the micelles was determined in the case of the dodecyl- and tridecyl-β-D-thiomaltobioside **8** and **10** by small-angle neutron scattering (SANS).

The shape of the distribution function (Fig. 8) calculated from the scattering data using the program GNOM (by D. Svergun, EMBL, Hamburg) suggests that some non-spherical aggregates are formed, since in the case of spherical micelles a Gaussian shaped distribution function would have been found. These results supported our hypothesis that the found phase might be a lyotropic cholesteric phase, and in the next step model calculations (for details, see Section 2.2) have been performed to simulate the SANS pattern of the two possible kinds of anisotropic micelles, disc-like micelles and cylindrical micelles. In Fig. 9 the experimental SANS data are shown, together with the model fits for the two different kinds of micelles. It can easily be seen that the experimental data match very well with the model fits for cylindrical micelles, and with this information the size of the micelles forming the lyotropic cholesteric phase of compounds **8** and **10** was calculated from the SANS data.

Compound **8**

Radius of cylinder 2.00 ± 0.01 nm, Length 29.0 ± 0.1 nm.

Compound **10**

Radius of cylinder 1.95 ± 0.01 nm, Length 29.0 ± 0.1 nm.

Since this phase was found more or less abundantly in the case of stearyl glycosides with a disaccharide headgroup, the question arose, as to whether or not its occurrence is restricted to this long chain compound. To answer this question, contact preparations using maltobiosides with a shorter alkyl chain were performed. In the case of the tetradecyl-β-D-maltobioside **36**, a lyotropic cholesteric phase was still found by polarising microscopy. This phase disappeared, if the tetradecyl chain was shortened by two CH_2-groups (dodecyl-β-D-maltobioside **35**). These compounds have also been analysed by small-angle neutron

diffraction (SANS). The SANS data of the tetradecyl-β-D-maltobioside **36** (Fig. 10 a) again matched well with the model fits for cylindrical micelles (the size of the micelles was calculated as above from the SANS data; length of the cylinders 20.0 nm, radius 2.0 nm), while the SANS data of dodecyl-β-D-maltobioside **35** do not (Fig. 10 b). These data match instead well with the model fit calculated for ellipsoidal micelles (again the size of the micelles was calculated from the SANS data; minor radius 2.0 nm, axis ratio 1.8). This result, together with the outcome of the contact preparations, can be interpreted in terms of a chain length-dependence of the occurrence of a lyotropic cholesteric phase. This phase can only be found beyond a minimum chain length, which in the case of the alkyl-β-D-maltobiosides proved to be a tetradecyloxy chain. Below this chain length, only slightly unisotropic ellipsoidal micelles are formed which do not adopt a lyotropic cholesteric phase. The reason for this chain length dependence might be seen in constraints to the formation of unisotropic micelles, due to problems filling the hydrophobic volume of the anisotropic micelles in the case of short alkyl chains.

The α cellobioside **12** formed on cooling of the melted sample the already described monotropic cubic phase, which was brought into contact with water. With increasing water concentration, a lamellar phase formed, followed by another cubic phase, a columnar phase, and a lyotropic cholesteric phase at the highest water concentration, and the phase sequence is, therefore, V_{II}, L_{α}, V_I, H_I, ch. From this contact preparation, it can be concluded that the thermotropic cubic phase of the cellobioside **12** should also be of the inverted type of bicontinuous cubic phases (see also Section 3 above), and the same holds true for the monotropic cubic phases of the lactobiosides **16** and **18**, since the reason for the formation of this monotropic cubic phase — i.e. a linear structure with an extremely imbalanced ratio between the hydrophilic and hydrophobic moieties — is the same. After penetration with water, the lactobiosides **16** and **18** formed with increasing water concentration only a cubic, a columnar and probably also a lyotropic cholesteric phase, i.e. the phase sequence was V_I, H_I, and ch. Within the cubic phase, a sharp boundary could be seen,

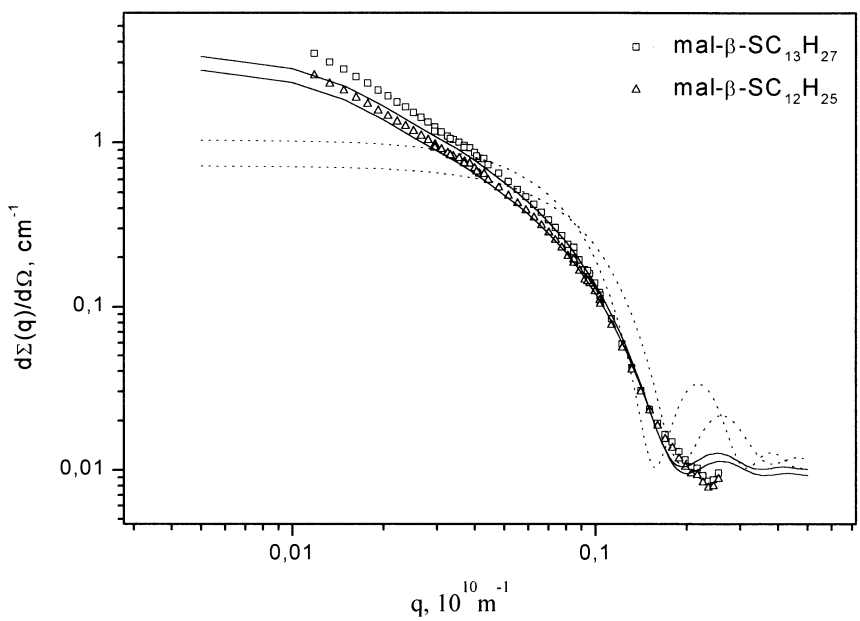

Fig. 9. SANS data for compounds **8** and **10** together with the model fits; solid lines, model fits for cylindrical micelles; dashed lines, model fits for disc-like micelles.

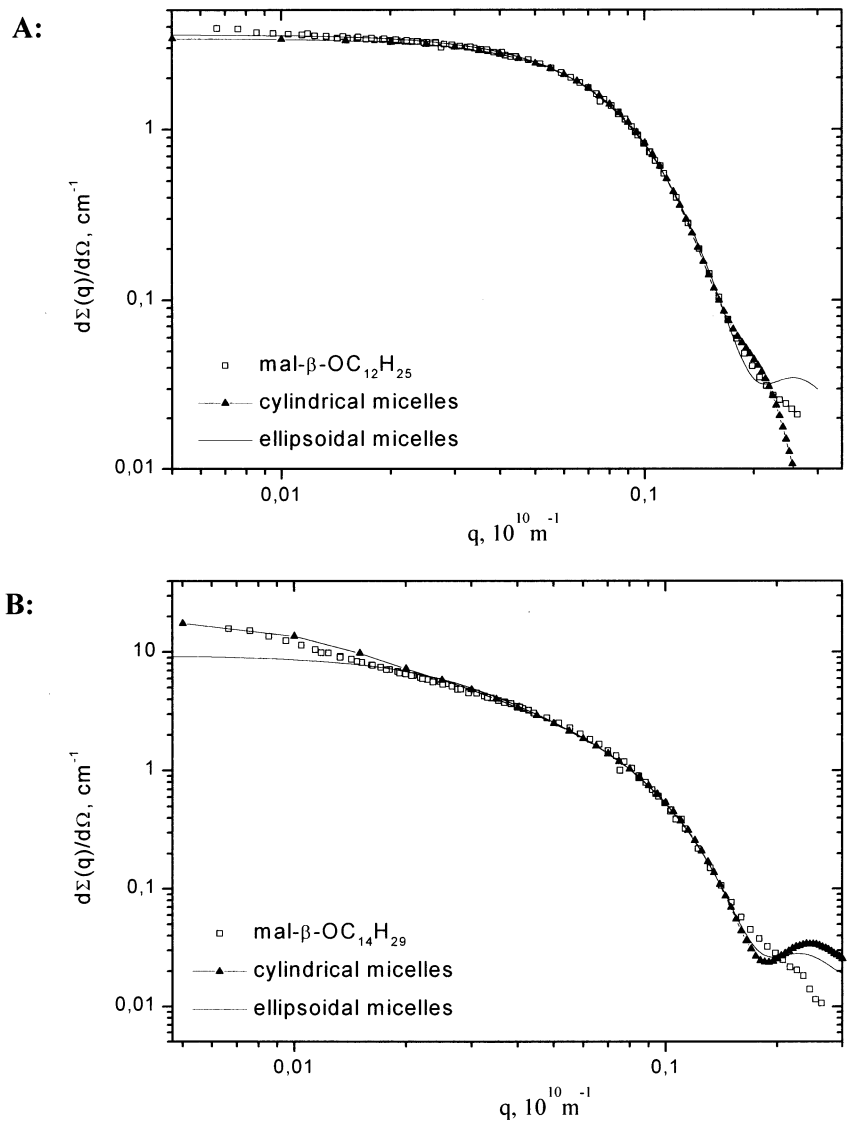

Fig. 10. SANS data and model fits for, (A) SANS data for mal-β-$OC_{12}H_{25}$ (**35**) together with model fits for cylindrical and ellipsoidal micelles; (B) SANS data for mal-β-$OC_{14}H_{29}$ (**36**) together with model fits for cylindrical and ellipsoidal micelles.

separating two isotropic regions. Since no lamellar phase was formed as in the case of the cellobioside **12**, it is impossible to decide whether the inner isotropic region is of the inverted cubic V_{II} type or a cubic glass, which has formed out of the cubic phase on cooling. The formation of a cubic glass on cooling could also account for the disappearance of the additional lamellar L_α phase.

Since the boundary of the H_I phase towards the water region was somewhat diffuse in the case of the lactobiosides, the existence of a lyotropic cholesteric phase, normally forming a thin weakly anisotropic band besides the columnar phase, could not be proved unambiguously by polarising microscopy. However, this seems very likely.

The β cellobioside **14**, which crystallised much

better than the α cellobioside **12**, formed only an L_α phase, a H_I phase, and a lyotropic cholesteric phase with water.

The stearyl-α-melibioside **20** formed with increasing water concentration a lamellar L_α phase, followed by a region where crystallisation occurred, followed by a cubic V_I phase, a columnar H_I phase, and a lyotropic cholesteric phase at the highest water concentration. For the β anomer **22**, the same phase sequence was observed except for the bicontinuous V_I phase, which disappeared completely while the region, where crystallisation occurred, broadened. The explanation for this behaviour might again be the greater tendency, mentioned already, of the compounds with a β-linked aliphatic chain to crystallise.

On penetration with water, the cubic phase of dodecyl-α-melibioside **26** developed a columnar phase followed by two isotropic regions separated from each other by a sharp border. These isotropic phases in the contact preparation beyond the H_I phase towards higher water concentration are, according to the general phase behaviour of amphiphiles, supposed to be micellar cubic phases, i.e. the phase sequence is V_I, H_I, I_I, I_{I*}, but it is rather unusual that two of them are found and in the case of the β anomer, the second discontinuous cubic phase disappeared. This different behaviour must be attributed to the different linkage of the aliphatic chain to the melibiose headgroup, yielding in the case of the α anomer an even broader banana-shaped structure than in the case of the β anomer.

3.2.2. Fourier-transform infrared spectroscopy

The $L_\beta \leftrightarrow L_\alpha$ alkyl chain melting was determined IR-spectroscopically via the $\nu_s(CH_2)$-vibration. The phase transition temperatures of the thio maltobiosides and melibiosides **8**, **10**, **26**, and **28** with short lipid chains (C12 and C13) lie in the range $< 0–7$°C, i.e. there are only slight differences between the O- and S-containing samples (Fig. 11a). The different wavenumber values corresponding to different states of order in the respective phase states are noteworthy. This relates in particular for the melibiosides, which are in the α-linkage more fluid (higher wavenumbers) than in the ß-linkage. As should be expected, the T_c-values of the C18-containing samples are much larger than those with shorter alkyl chains (Fig. 11b). However, the kind of disaccharide and the nature of the linkage strongly influences the T_c-value. For example, regarding the stereoisomeric stearyl melibiosides and lactosides, the T_c–value of the latter as well as their state of order is much higher than that of the former (Fig. 11b). For the melibiosides, the T_c-values are 38 and 67.5°C in α- and β-linkage (**20** and **22**), respectively.

3.3. Synchrotron radiation X-ray diffraction

The three-dimensional aggregate structures are also strongly dependent on the sugar- and linkage-types. The results for the dodecyl melibiosides (**26** and **28**) and the dodecyl and tridecyl thiomaltosides (**8** and **10**) with short alkyl chains are presented in Fig. 12. The scattering curves basically consist of two broad intensity maxima around 0.1 and 0.25–0.30 nm, which might be interpreted as typical for unilamellar structures (Worthington and Khare, 1978; Bouwstra et al., 1993). For the maltosides, above 40°C, sharp reflections occur, which could be typical for multilamellar aggregation. However, the 'normal' bilayer L phase can be excluded, because in that case, the periodicities should be much higher (for a maltose-containing ether-linked C14-dialkylglycolipid, Hinz et al. (1991) found values above 6 nm). Therefore, an interdigitation of the alkyl chains may be assumed similarly as found recently for stearyl monosaccharides (Vill et al., in press), for these, however, only in the gel phase.

The samples with a C-18 chain and the different disaccharides maltose, melibiose, cellobiose, and lactose as headgroup exhibit a much more complex structural polymorphism. The broad diffraction maxima indicate the existence of unilamellar structures, except for the ß-linked maltobioside **4**. The latter undergoes two phase changes (Fig. 13a). At 5°C, the two reflections at 6.22 and 3.58 nm are in a ratio of $\sqrt{3}$, indicating the absence of a lamellar phase, but rather the presence of the micellar H_I phase. Above 20°C, i.e. above the temperature of the 'pre-transition' (see Fig. 11), clearly a multilamellar structure can be observed. Another structural change occurs above 60°C, the diffraction patterns at 80°C expressing a strong increase of the main peak to 5.59 nm and an occurrence of two new

reflections at 4.55 and 2.75 nm. These numbers, however, are not interconnected by a particular numerical relation as found in lamellar or cubic structures indicating possibly the superposition of different structures. From Fig. 13a, it becomes clear that the stereoisomeric maltoside and cellobioside behave quite differently, emphasising the importance of the kind of anomeric linkage.

The melibiose-containing α-linked sample exhibits complex diffraction patterns between 5 and 40°C (Fig. 13b), which may be due to a cubic structure (e.g. the relations hold 3.59 nm = 12.5 nm/$\sqrt{12}$, and 2.77 nm = 12.5 nm/$\sqrt{20}$). Above $T_c = 40$°C, the structure converts into a different, possibly unilamellar one. The shape of the broad diffraction maxima indicates, however, that another unresolvable structure may be superimposed. A similar polymorphism like that of the

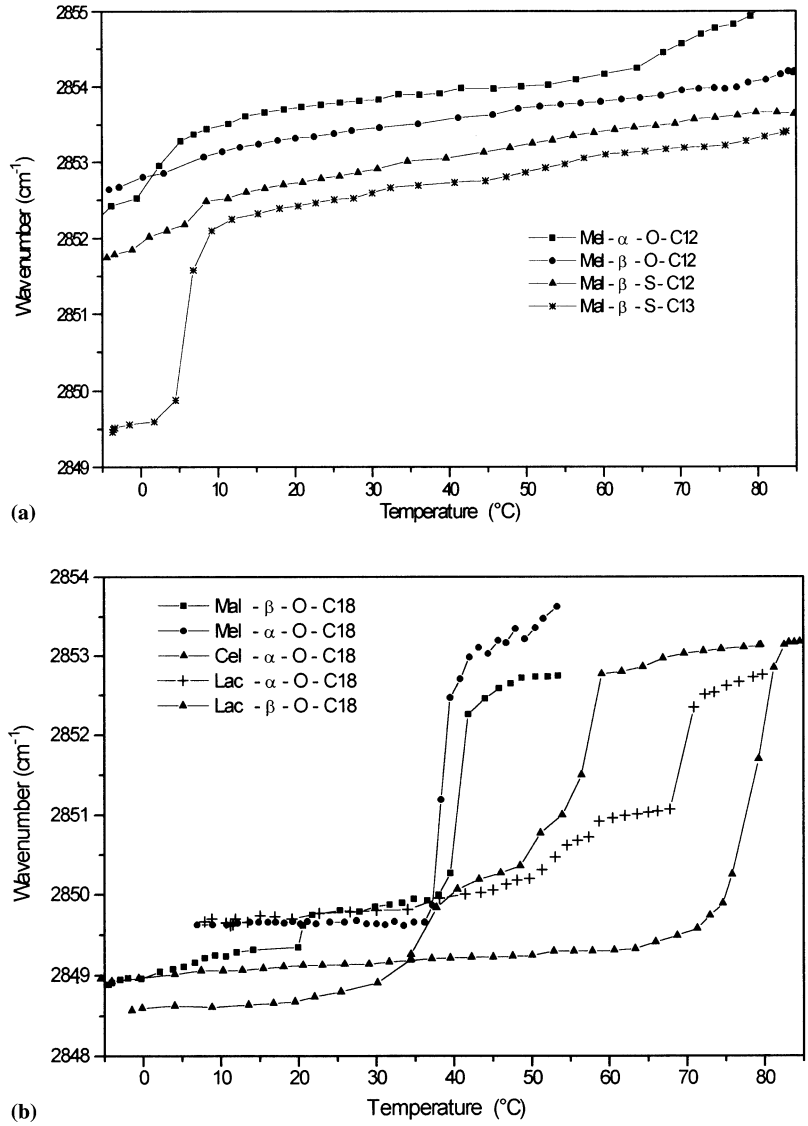

Fig. 11. Peak position of the symmetric stretching vibration of the methylene groups $\nu_s(CH_2)$ vs. temperature for various, (a) short-chain disaccharide glycolipids; and (b) stearyl-disaccharide glycolipids.

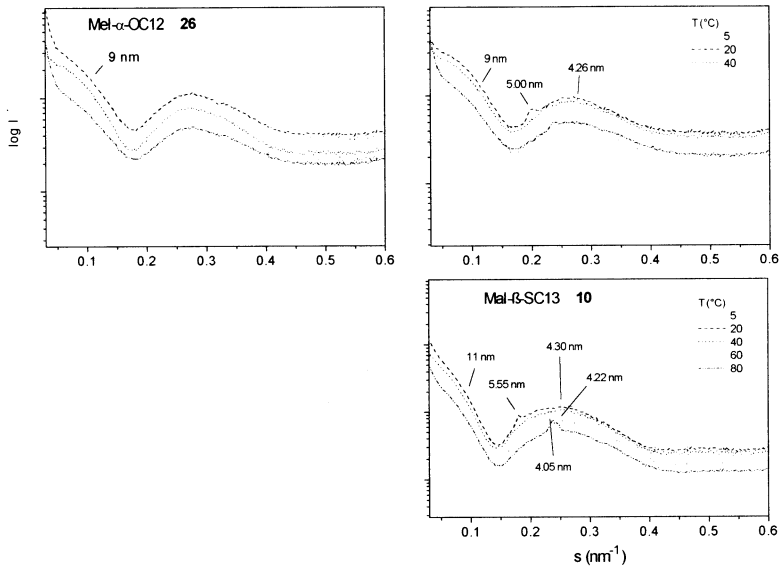

Fig. 12. Small-angle X-ray diffraction patterns for various short-chain disaccharide glycolipids in the temperature range 5–80°C. Water content, 90%.

latter sample is expressed by the cellobiose-containing compound, the only difference is the higher temperature at which the change into a mainly unilamellar phase occurs, corresponding to the higher value of $T_c = 55°C$.

The two lactosides exhibit a very similar behaviour over the entire temperature range (data not shown). The patterns might be interpreted as resulting from lamellar structures — the broadness of the peaks indicates a low number of lamellae. However, a jump of the peak maximum to higher values (4.76 and 4.65 nm, respectively) at $T_c = 70°C$ is observed, which does not indicate a pure $L_ß \leftrightarrow L_\alpha$ transition, because this should be accompanied by a decrease rather than an increase of the periodicity. The latter observation could be consistent with a transition from a lamellar into a non-lamellar phase as previously found for lipid A from *Salmonella minnesota* for the $L \leftrightarrow H_{II}$ transition (Brandenburg et al., 1998).

For some of these glycosides, also wide-angle X-ray diffraction experiments were performed to determine the short-range order, i.e. the packing of the alkyl chains, particularly in their gel phase. It was found that, for example, for the two melibiosides the α-anomer has a reflection at 0.451 nm, whereas that of the β-anomer is centred at 0.420 to 0.424 nm, indicating, in accordance to the infrared data, a higher order of the latter anomeric configuration. Table 1 summarises the results of the infrared spectroscopic and the X-ray diffraction experiments. In accordance with the microscopic contact preparations, cel-α-OC18 **12** forms a cubic phase, whereas for the lactosides only lamellar phases are observed in contrast to the contact preparation. For an understanding, it should be considered that the X-ray data were obtained at a much higher (90%) water content than in the microscopic preparations (see lyotropism). The reduction of the water concentration in X-ray diffraction experiments to 55% gave results very similar to those obtained at 90% buffer content, i.e. a lyotropic phase behaviour as described above should play a role only at water concentrations below 50%.

Although the investigated disaccharide headgroups exclusively consist of a 'glu–glu' or 'glu–gal' compound, an enormous diversity of structural polymorphism (alkyl chain melting and order, types of aggregate structures) are observed

dependent of the kind of sugars and of the anomeric linkage to the acyl chain and within the two sugars. These observations might give an idea for an understanding of the complex biological functions of such glycolipids in nature.

Acknowledgements

We are grateful for financial support from the *Deutsche Forschungsgemeinschaft* (SFB 470, projects B5 and B6).

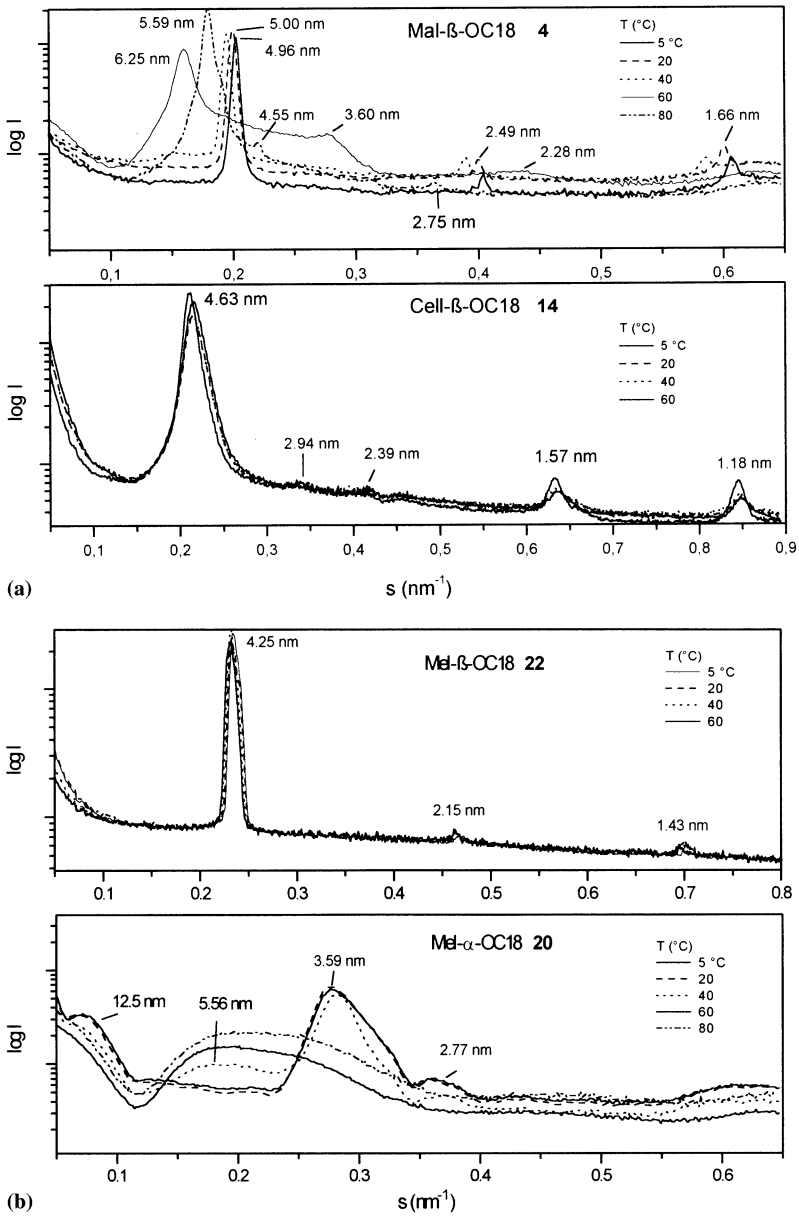

Fig. 13. Small-angle X-ray diffraction patterns in the temperature range 5–80°C for, (a) the stereoisomers maltoside and cellobioside in β-linkage; and (b) the two melibioside anomers. Water content, 90%.

References

Beginn, U., Keinath, S., Moeller, M., 1997. Liq. Cryst. 23, 35–41.

Blunk, D., Praefke, K., Vill, V., 1998. Amphotropic liquid crystals. In: Demus, D., Goodby, J., Gray, G.W., Spiess, H.-W., Vill, V. (Eds.), Handbook of Liquid Crystals, vol. 3. Wiley-VCH, Weinheim, pp. 305–340.

Böcker, T., Thiem, J., 1989. Synthese und eigenschaften von kohlenhydrattensiden. Tenside Surf. Det. 26, 318–324.

Borisch, K., Diele, S., Göring, P., Müller, H., Tschierske, C., 1997. Amphiphilic *N*-benzoyl-1-amino-1-deoxy-D-glucitol derivatives forming thermotropic lamellar, columnar and different types of cubic mesophases. Liq. Cryst. 22, 427–443.

Bouligand, Y., 1998. Defects and textures. In: Demus, D., Goodby, J., Gray, G.W., Spiess, H.-W., Vill, V. (Eds.), Handbook of Liquid Crystals, vol. 1. Wiley-VCH, Weinheim, pp. 406–453.

Boulin, C., Kempf, R., Koch, M.H.J., McLaughlin, S.M., 1986. Data appraisal, evaluation and display for synchrotron radiation experiments: hardware and software. Nucl. Instr. Methods A249, 399–407.

Boullanger, P., 1998. Amphiphilic carbohydrates as a tool for molecular recognition in organized systems. In: Drigenz, H., Thiem, J. (Eds.), Topics in Current Chemistry, vol. 187. Springer, Berlin Heidelberg, pp. 275–312.

Brandenburg, K., Koch, M.H.J., Seydel, U., 1990. Phase diagram of lipid A from *Salmonella minnesota* and *Escherichia coli* rough mutant lipopolysaccharide. J. Struct. Biol. 105, 11–21.

Brandenburg, K., Richter, W., Koch, M.H.J., Meyer, H.W., Seydel, U., 1998. Characterization of the nonlamellar cubic and H_{II} structures of lipid A from *Salmonella enterica* serovar *minnesota* by X-ray diffraction and freeze-fracture electron microscopy. Chem. Phys. Lipids 91, 53–69.

Casal, H.L., Mantsch, H.H., 1984. Polymorphic phase behaviour of phospholipid membranes studied by infrared spectrosopy. Biochim. Biophys. Acta 779, 381–401.

Curatolo, W., 1987. The physical properties of glycolipids. Biochim. Biophys. Acta 906, 111–136.

Dahlhoff, W.V., 1987. Amphiphilic carbohydrate-based mesogens 2, aldose di-n-alkyl dithioacetals: novel double-tailed thermotropic liquid crystals. Z. Naturforsch. 42b, 661–662.

Dahlhoff, W.V., 1990. Synthesis of a series of alkyl 1-tio-D-glucopyranosides and their regioselective reductions to 1-alkylthio-1-deoxy-D-glucitols. Liebigs Ann. Chem., 1025–1027.

Eckert, A., Kohne, B., Praefcke, K., 1987. Flüssigkristalline kohlenhydratdithioacetale. Z. Naturforsch. 43b, 878–888.

Ellens, H., Siegel, D.P., Alford, D., Yeagle, P.L., Boni, L., Lis, J., Quinn, P.J., Bentz, J., 1989. Membrane fusion and inverted phases. Biochemistry 28, 3692–3703.

Fairhurst, C.E., Fuller, S., Gray, J., Holmes, M.C., Tiddy, G.J., 1998. Lyotropic surfactant liquid crystals. In: Demus, D., Goodby, J., Gray, G.W., Spiess, H.-W., Vill, V. (Eds.), Handbook of Liquid Crystals, vol. 3. Wiley-VCH, Weinheim, pp. 341–392.

Fischer, E., Helferich, B., 1911. Über neue synthetische glycoside. Liebigs Ann. Chem. 383, 68–91.

Fischer, S., Fischer, H., Diele, S., Pelzl, G., Jankowski, K., Schmidt, R.R., Vill, V., 1994. On the structure of the thermotropic cubic mesophase. Liq. Cryst. 17, 855–861.

Gabriel, A., Dauvergne, F., 1982. The localization method used at EMBL. Nucl. Instr. Methods 201, 223–224.

Glatter, O., 1977. Data evaluation in small angle scattering: calculation of the radial electron density distribution by means of indirect Fourier transformation. Acta Phys. Aust. 47, 83–102.

Glatter, O., 1992. Mathematical, physical and chemical tables. In: Wilson, A.J. (Ed.), International Tables for Crytalography. Kluwer Academic Publishers, Dordrecht.

Glatter, O., Kratky, O. (Eds.), 1982. Small-Angle X-ray Scattering. Academic Press, London, p. 431.

Hori, R., 1958. Alkylderivatives of carbohydrates. II. Synthesis of alkyl-β-cellobiosides. Yakugaku Zasshi 78, 999–1002.

Israelachvili, J.N., 1991. Intermolecular and Surface Forces. Academic Press, London.

Jeffrey, G.A., 1984. Carbohydrate liquid crystals. Mol. Cryst. Liq. Cryst. 110, 221–237.

Jeffrey, G.A., Wingert, L.M., 1992. Carbohydrate liquid crystals. Liq. Cryst. 12, 179–202.

Koch, R., 1884. Die aetiologie der tuberkulose. Mitt. K. Gesundheitsamt. 2, 1–88.

Koynova, R., Caffrey, M., 1994. Phases and phase transitions of the glycoglycerolipids. Chem. Phys. Lipids 69, 181–207.

Lindblom, R., Rilfors, R., 1989. Cubic phases and isotropic structures formed by membrane lipids — possible biological relevance. Biochim. Biophys. Acta 988, 221–256.

Luzzati, V., Gulik, A., Gulik-Krzywicki, T., Tardieu, A., 1986. Lipid polymorphism revisited: structural aspects and biological implications. In: Lipids and Membranes: Past, Present, and Future. Elsevier, Amsterdam, pp. 137–151.

Mannock, D.A., Lewis, R.N.A.H., McElhaney, R.N., 1987. An improved procedure for the preparation of 1,2-di-*O*-acyl-3-*O*-(β-D-glucopyranosyl)-*sn*-glycerols. Chem. Phys. Lipids 43, 113–127.

Mannock, D.A., Lewis, R.N.A.H., McElhaney, R.N., 1990. The chemical synthesis and physical characterisation of 1,2-di-*O*-acyl-3-*O*-(α-D-glucopyranosyl)-*sn*-glycerols, an important class of membrane glycolipids. Chem. Phys. Lipids 55, 309–321.

Niori, T., Sekine, T., Watanabe, J., Furukawa, T., Takezoe, H., 1996. J. Mater. Chem. 6, 1231–1233.

Pedersen, J.S., 1997. Analysis of small-angle scattering data from colloids and polymer solutions: modelling and least-squares fitting. Adv. Colloid Interface Sci. 70, 171–210.

Prade, H., Miethchen, R., Vill, V., 1995. Thermotrop flüssigkristalline kohlenhydrat-amphiphile. J. Prakt. Chem. 337, 427–440.

Praefcke, K., Kohne, B., Eckert, A., Hempel, J., 1990. Inososе-flüssigkristalle. Z. Naturforsch. 45b, 1084–1090.

Rosevar, P., VanAken, T., Baxter, J., Ferguson-Miller, 1980. Alkyl glycoside detergents: a simple synthesis and their effects on kinetic and physical properties of cytochrome c oxidase. Biochim. Biophys. Acta 19, 4108–4115.

Seddon, J.M., 1990. Structure of the inverted hexagonal (H_{II}) phase, and non-lamellar phase transitions of lipids. Biochim. Biophys. Acta 1031, 1–69.

Seydel, U., Labischinski, H., Kastowsky, M., Brandenburg, K., 1993. Phase behaviour, supramolecular structure, and molecular conformation of lipopolysaccharide. Immunobiology 187, 191–211.

Siegel, D.P, 1986a. Inverted micellar intermediates and the transition between lamellar, cubic and inverted hexagonal lipid phases; I. Mechanism of the L_a-H_{II} phase transition. Biophys. J. 49, 1155–1170.

Siegel, D.P, 1986b. Inverted micellar intermediates and the transition between lamellar, cubic and inverted hexagonal lipid phases; II. Implications for membrane–membrane interactions and membrane-fusion. Biophys. J. 49, 1171–11783.

Siegel, D.P, 1986c. Inverted micellar intermediates and the transition between lamellar, cubic and inverted hexagonal lipid phases; III. Isotropic and inverted cubic state formation via intermediates in transitions between L_a and H_{II} phases. Chem. Phys. Lipids 42, 279–301.

Siegel, D.P., Banschbach, J., Alford, J., Ellens, H., Lis, L.J., Quinn, P.J., Yeagle, P.L., Bentz, J., 1989. Physiological levels of diacylglycerols in phospholipid membranes induce membrane fusion and stabilize inverted phases. Biochemistry 28, 3703–3709.

Stuhrmann, H.B., 1989. Small-angle scattering of X-rays. In: Progress Crystal Growth and Characteristics, vol. 18. Pergamon Press, Oxford, pp. 1–18.

Stuhrmann, H.B., Burkhardt, N., Dietrich, G., Jünemann, R., Meerwinck, W., Schmitt, M., Wadzack, J., Willumeit, R., Zhao, J., Nierhaus, K.H., 1995. Proton- and deuteron-spin targets in biological structure research. Nucl. Instr. Methods A356, 133–137.

Tietze, L.F., Böge, K., Vill, V., 1994. Liquid-crystalline D-glucose dialkyl acetals and dodecyl D-glucofuranosides. Chem. Ber. 127, 1065–1068.

Van Doren, H.A., Wingert, L.M., 1994. The relationship between the molecular structure of polyhydroxy amphiphiles and their aggregation behaviour in water; I. The contact preparation method as a tool for empirical studies. Recl. Trav. Chim. Pays-Bas 113, 260–265.

Van Doren, H.A., Buma, T.J., Kellog, R.M., Wynberg, H., 1988. Carbohydrate liquid crystals even at ambient temperature. J. Chem. Soc. Chem. Commun., 460–462.

Van Doren, H.A., van der Geest, R., Kellogg, M.K., Wynberg, H., 1989. Synthesis and liquid crystalline properties of the n-alkyl 1-thio-α-D-glucopyranosides, a new homologous series of carbohydrate mesogens. Carbohydr. Res. 194, 71–77.

Van Doren, H.A., van der Geest, R., Kellogg, M.K., Wynberg, H., 1990. A comparative study of the liquid-crystalline behavior of three homologous series of 1,2-propanediol derivatives. Recl. Trav. Chim. Pays-Bas 109, 197–203.

Vill, V., 1999. LiqCryst 3.3-database of liquid crystalline compounds for personal computers. Fujitsu Kyushu Systems (FQS) Ltd., Fukuoka, Japan; LCI Publisher, Hamburg, 1999. http://liqcryst.chemie.uni-hamburg.de

Vill, V., Böcker, T., Thiem, J., Fischer, F., 1989. Studies on liquid crystalline glycosides. Liq. Cryst. 6, 349–356.

Vill, V., Kelkenberg, H., Thiem, J., 1992. Liquid-crystalline glucamin derivatives. Liq. Cryst. 11, 459–467.

Vill, V., v. Minden, H. M., Koch, M. H. J., Seydel, U., Brandenburg, K., 1999. Thermotropic and lyotropic properties of long chain alkyl glycopyranosides. Part I: monosaccharide headgroups. Chem. Phys. Lipids, in press.

Vogel, C., Jeschke, U., Vill, V., Fischer, H., 1992. D-Galacturonsäurederivate mit flüssigkristallinen eigenschaften. Liebigs Ann. Chem., 1171–1177.

Wignall, G.D., Bates, F.S., 1986. Absolute calibration of small-angle neutron scattering data. J. Appl. Cryst. 20, 28–40.